An early method for the technical diagnosis of pin-on-disk tribometers by reference friction measurements in EHL conditions

An early method for the technical diagnosis of pin-on-disk tribometers by reference friction measurements in EHL conditions

Edoardo Goti[1], Luigi Mazza[1], Andrea Mura[1], Bin Zhang[2]

[1] Department of Mechanical and Aerospace Engineering, Politecnico di Torino, Corso Duca degli Abruzzi 24, 10129 Torino, ITALY
[2] Anton Paar TriTec, Les Vernets 6, 2035 Corcelles-Cormondrèche, SWITZERLAND

Abstract

Reference tests are widely used to calibrate scientific instruments but are potential candidate to establish technical diagnosis procedures for scientific instruments too. A reference test is currently lacking in tribology. Though, it would allow users to check that tribometers are properly working and may also form a yardstick for cross-laboratory comparative studies. In this paper two easy-to-use reference testing procedures for the diagnosis of commercial pin-on-disc tribometers are established resorting to a special no-wear test setup in EHL conditions. Several tests were carried out with two tribometers and two commercial oils, and both standardized testing modes were investigated: unidirectional-rotating and linear-reciprocating mode. The friction curves from more than 350 tests were analyzed to generate meaningful statistics supporting the robustness of these procedures. The test setup proved to be suitable for the task since the summary of the results showed an excellent repeatability of friction curves concerning appearance and average values

Highlights

- A novel reference test procedure is proposed for the pin-on-disc tribometers technical diagnosis
- The EHL condition is exploited to obtain stable and highly repeatable friction curves
- A user-friendly lubricated test setup is put in place in order to fit industrial applications
- Measurements are performed with 2 tribometers in 2 laboratories, then analyzed and compared

Keywords
Friction; Pin-on-disk; Diagnostics; Tribometer; Reference test; EHL

Abbreviations and Nomenclature

AAV	Average of the average coefficient of friction values
ASt.DV	Mean of the standard deviation values of coefficient of friction
CoF	Coefficient of friction
E’	Composite elastic modulus
E_b	Ball elastic modulus
E_d	Disc elastic modulus
EHL	Elastohydrodynamic lubrication
F_N	Normal load
F_T	Tangential friction force
G	Dimnesionless material parameter for EHL equations
G_V	Dimensionless Hamrock’s viscosity parameter
G_E	Dimensionless Hamrock’s elastic parameter
HVo	High viscosity oil
k	Ellipticity factor
Λ	Lambda (or roughness) factor
L	Material parameter (Moes); $L= G\cdot(2U)^{0.25}$
M	Load parameter (Moes); $M= W / (2U)^{0.75}$
MVo	Middle viscosity oil
R’	Composite curvature radius of mating surfaces
R_b	Ball radius
R_d	Disc radius

SRR	Slide-to-roll ratio
St.DAV	Standard deviation of the average coefficient of friction values
U	Dimensionless speed parameter for EHL equations
$\bar{U}$	Entrainment speed
v_b	Ball linear speed
v_d	Disc linear speed
VI	Viscosity index
α	Pressure-viscosity coefficient
α_T	Temperature-viscosity coefficient
η_0	Dynamic pressure in atmospheric conditions;
ν_b	Ball Poisson ratio
ν_d	Disc Poisson ratio
W	Dimensionless load parameter for EHL equations

---

1. Introduction

It is well known that the coefficient of friction (CoF) of a tribological pair is far from being only a characteristic property of the materials involved into the contact[1] since it also depends on many other parameters: speed, load, temperature, humidity, wear, size/scale…to name but a few [2]. In such a scenario, the test rig itself is also expected to affect the estimation of the coefficient of friction, as a result of its mechanical layout, its own dynamic characteristic and the specific test set-up and contact geometry. Therefore, no experimental value of the coefficient of friction can ever be stated as "representative" or "correct" in absolute terms. Precisely for these reasons the DIN 50322 standard accepts, for example, that friction results from "model tests" (i.e. typical simplified laboratory tests, including pin-on-disc) may be very different compared to the results from "field tests" (i.e. tests in actual operating conditions) even if similar materials or components are involved. The ASTM G99 standard, the referral standard for pin-on-disc method, also warns that there is no ensurance the tests will predict the behavior of a given material in actual application under conditions differing from those in the test.

In the field of tribology results are usually scattered and it is not obvious to find consistent results under the same testing conditions, especially in dry testing conditions were the materials wearing-out process introduces uncertainties. The results of the Interlaboratory tests included in the ASTM G99 standard are themselves rather scattered, unsuited to represent a reference because of wear. Moreover, very often average values and coefficients of variations for CoF are shown without even disclosing actual friction curves, which can vary a lot when repeating merely the same test although average values are similar. Nonetheless, should one be able to measure consistent friction curves (let us call it an "usual" result) under the same conditions, over time and across different tribo-testing machines of the same kind, such conditions may form, at least, a relative reference. By extension, a reference test may be established and a criterion to assess if one particular tribometer is potentially affected by technical problems can be derived by comparison of the specific outcome with the one usually expected. This approach conforms indeed to ISO 13372:2012 which defines the attitude of technical diagnosis to collect data and information (i.e. condition monitoring [3]) to detect problems and deviations from normal conditions.

The aim of this experimental investigation is therefore to develop a reference procedure for pin-on-disk tribometers based on reference tests featuring a stable and repeatable characteristic coefficient of friction. This

procedure would include one reference test intended for unidirectional rotating mode and one for linear reciprocating mode. In order to achieve this challenging result, this paper explores a special no-wear test setup in elastohydrodynamic lubricated conditions and its peculiar friction performances. The authors wish to demonstrate the reliability of the chosen method which is then proposed as a monitoring and diagnostic tool for tribometers, able to make an assessment on either software / hardware issues or issues in terms of calibration. The method qualifies as Structural Health Monitoring (SHM) [3] applied to a very special mechanical system, i.e. a scientific instrument, where friction force itself acts as the monitoring parameter for which a reference value is available. In pin-on-disk tribometers the CoF is calculated following the classical definition: $\mu = F_T/F_N$ where the quantity that is measured is indeed the tangential friction force F_T acting at the contact area, and F_N is a known normal force.

In the last 60 years a lot of scientific works have investigated the elastohydrodynamic lubrication(herein referred to as EHL or EHD) whose theoretical foundations were laid by Grubin [4], Dowson and Higginson [5] and Hamrock and Dowson [6]. EHL is a contact mode typical of lubricated non-conformal contacts. It is the typical contact condition found in machine elements interacting under low geometrical conformity, where loads act over relatively small contact areas, such as the point contacts of ball bearings and the line contacts of roller bearings and of gear teeth. EHD phenomena also occur in some low elastic modulus contacts, such as lip seals [7]. Among them, a multitude of papers have investigated the coefficient of friction in EHL point contacts. However, all these works focused either on several aspects of lubrication modes or the development/optimization of numerical models for specific experimental cases or specific applications. In almost everyone a ball-on-disc test rig designed on purpose was used. Test rigs for interferometric film thickness measurements are typically used when the aim is to correlate friction with lubrication regimes and plot the Stribeck curve. For example, friction values measured in this way were reported in the works by Zhang et al. [8],[9], Fu et al. [10], [11] and Ciulli et al. [12], Carli et al. [13], Gunsel et al.[14], Nishikawa et al. [15] who investigated all lubricated conditions with testing parameters rather similar to those in this paper. Hansen et al. [16][17], Bjorling et al. [18]. Vengudusamy et al. [19] and Guegan et al. [20] reported the effects of roughness on traction coefficient (CoF) by mapping transitions of lubrication regimes. Hansen et al. supported also interferometric observations with electric contact resistance (ECR) technique. Also, Nishikawa et al. [21] and Han et al. [22] investigated friction phenomena in reciprocating sliding motion with a test rig of the same kind. Ball-on-disc traction test rigs are often resorted to when the evolution of traction coefficient is studied in response to the variation of the slide-to-roll ratio. With regard to this, it is worth to cite the work by Vegudusamy et al. [23] and Angel et al. [24]. Schwing-Reib-Verschleiss (SRV) tribometers are sometimes used too, for example in the same papers by Vegudusamy et al. [23] and Han et al. [22]. Only some authors in the scientific literature dealt with the friction behavior in lubricated conditions with pin-on-disk tribometers, like Anderson [25] and Podgornik [26] and Grützmacher [27]. Anderson performed lubricated tests with a classical pin-on-disk tribometer, he used a quite particular experimental set-up where water was used as lubricant and large amount of wear was unavoidable. Grützmacher tested a steel-steel friction pair in ball-on-disc lubricated conditions with testing parameters (rotational speed, track radius and load) very similar to those used for this study. However, he used much lower viscosity oils and focused on the transition from fully-flooded to mixed lubrication because of centrifugal forces at varying track radii. Muller and Ostermayer [28] used a High Load Tribometer (HLT), which basically consists of a pin on disk set-up, to study the problem of starvation in hydrodynamic lubrication of conformal contacts. Bai et al. [29] measured traction by means of a multi-purpose

tribometer in linear reciprocating pin-on-disk configuration. Kovalchenko et al. [30] measured a number of Stribeck curves with a pin-on-disc investigating the hydrodynamic lubricated contact with a flat pin though. To the best of the authors' knowledge, no other author has ever attempted to introduce a reference test or reference procedure in the tribology field to verify the testing apparatus itself, neither exploiting the EHD lubrication or another contact condition as a mean (rather than an end).

For the purpose of robust reliable statistics, the results from two pin-on-disk tribometers located in two different laboratories and in different environmental conditions were compared in this paper.

An empirical approach was basically followed in this study. No in-depth examination of the contact mechanics, and no experimental lubricant film thickness measurements are provided here as it goes beyond the scope of this paper. Yet, application of the available EHL equations is briefly presented in the next sections. This is just to support experimental evidence by checking that the predicted lubricant film thickness with the chosen testing parameters is in line with a no-wear EHL regime, leastwise.

The results presented hereafter are to be intended as preliminary results which need further verifications and a wider statistical base for acceptance as standard procedure.

2. Materials and Methods

The present experimental campaign was made possible thanks to the collaboration of the Department of Mechanical and Aerospace Engineering Laboratory (DIMEAS) at Politecnico di Torino (Torino, IT) and Anton Paar TriTec (Corcelles-Cormondrèche, CH). A total of two different Anton Paar pin-on-disk tribometers were used: a TRB tribometer and a TRB^3 tribometer of next generation. Both the instruments are compliant with the ASTM G99 and ASTM G133 standards. Manufacturer's technical specifications of the two instruments are presented in Appendix A and their functional scheme is shown in Figure 1b.

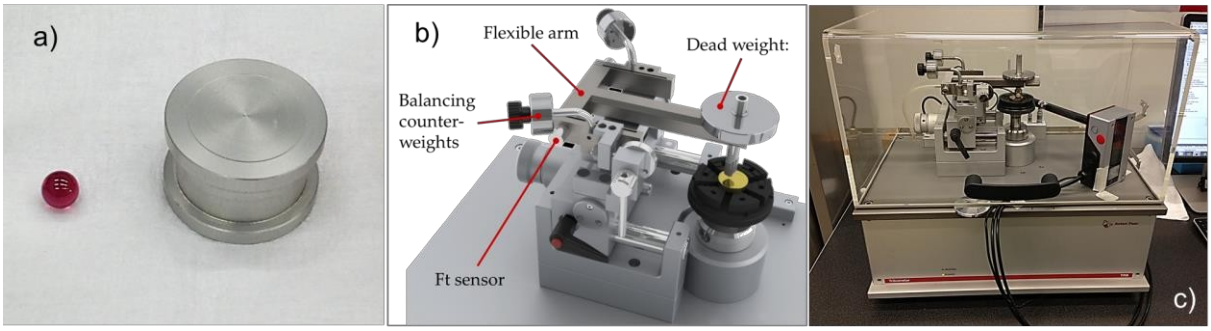

Figure 1. (a) Material pair for tests; (b) functional scheme of the Anton Paar pin-on-disk tribometers; (c) temperature and humidity sensor fitted inside the testing chamber

A lubricated contact is formed between a ruby ball (Saphirwerk AG, Brügg, CH) and a microscope round cover slip made of D263M ® borosilicate glass (Schott AG, Mainz, DE). Such a thin glass slip cannot be installed directly into the spindle clamping device as it is too fragile. To overcome this critical issue, the glass slip was glued on the top of an aluminum sample-holder (Figure 1a). Several samples were used, and the gluing of the

cover slip was handcrafted using fast-setting glue. The ball was mounted into a pin-shaped ball-holder thus pure sliding occurred at the interface (with a SRR [1] equal to 2).

Table I. Properties of the liquid lubricants and the tribological pair

OILS	Base stocks	Density [kg/dm^3]	Viscosity [cSt] @ 30°C	α [1] [GPa-1]	V.I. [2]
Anton Paar Testing Oil MV (MVo)	Semi-synthetic oil (Mineral oil and PAO base stocks)	0.861	122.2	30.5	101
Anton Paar Testing Oil HV (HVo)	Fully synthetic oil (PAO, Poly-1-decene, Polybutene base stocks)	0.839	740.3	34.8	123

MATERIAL PAIR	Elastic modulus [GPa]	Poisson ratio	Radius [mm]	Rq [µm]	Thickness [mm]
Ruby sphere	390	0.22	3	0.006	-
Glass cover slip	73	0.208	17	0.020	0.1

[1] Pressure-viscosity characteristics are calculated with So and Klaus' analytical model [31].
[2] Reference is made to the ASTM D2270 standard

Two types of commercial liquid lubricants were employed: a middle-viscosity and a high viscosity oil (herein referred to as MVo and HVo). Both are products of Anton Paar TriTec SA ad their main properties at the testing temperature are listed in Table I, together with the material properties of the sample pair. Both the oils are thermally stable, hydrophobic, resistant to atmospheric agents and characterized by a relatively high viscosity index (V.I.). Being commercial products, these lubricants come with their technical sheet certified by a meteorological laboratory. Tables of viscosity and other physical properties for the two oils are presented in Appendix B as provided in technical sheets. Viscosity values in Table I are interpolated via the popular Walters' formula considering the working temperature of 29°C.

The most widely used experimental techniques for testing lubricated contacts resort to either oil bath or continuous active or passive oil supply flow. In this study a little amount of oil was added on the top of the glass sample with a syringe before starting each test, as much to completely cover the surface region where the interaction between the solid surfaces takes place (Figure 2a).

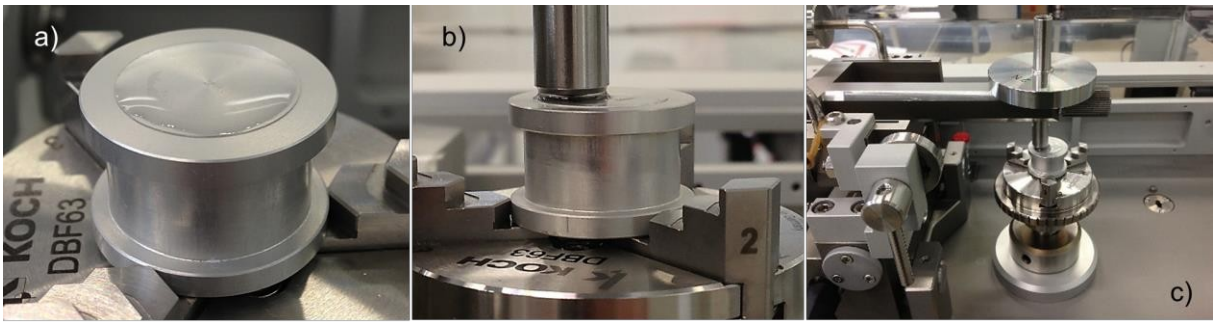

[1] Slide-to-roll ratio defined as: SRR = 2*(u_d - u_b)/(u_d + u_b), where 'd' stands for "disk" and 'b' for "ball"

Figure 2. (a) lubricant applied on the sample surface before a test; (b) zoomed view of the lubricated contact; (c) test set-up for rotating mode tests.

Bai et al. [29] reported successful full-film lubrication of sample surfaces by a very similar method without the system running into starved lubrication. More extreme techniques to supply lubricant to the contact region are also reported in the scientific literature. As an example, Li et al. [32] proved that lubrication by oil droplets supply is an effective way to form a continuous lubrication film at the contact region and avoid lubricant waste. Figure 2c shows the complete experimental set-up just before running a unidirectional rotating test and Figure 2b is a zoomed view of the lubricant meniscus during a test run.

The contact load was applied placing dead-weights on the measuring arm coaxially to the ball-holder. The tribometer vertical load range is 0.25N to 60N (see Appendix A). The MVo was selected for tests with relatively low vertical load, so as to explore the lower part of the instruments load range; the HVo was used for tests with higher vertical load so as to explore the higher part of the load range of the instruments. Preliminary tests allowed to identify the most favorable testing parameters. As to rotating tests, 1N and 2N loads have been tried out at 100rpm with the MVo. Tests under 1N and 2N yielded very similar results in terms of average CoF, but more regular curves showed up in the case of 2N load. Possible reasons for a higher regularity with higher normal load are system vibrations which are more negligible with higher loads and the lower influence of roughness as a result of a slightly greater contact area. As to the HVo, the desired load parameter was 60N at first, i.e. the upper bound of the instruments load range. However, after preliminary tests under load of 30N to 60N, coupled with speeds from 100rpm to 200rpm, none of the loads higher than 30N guaranteed complete separation between solid surfaces and the lubricating film ran systematically into failure with the glass slip breakup. On the contrary, test runs under 30N load and 150rpm yielded enough repeatability to give rise to a reference condition.

Some of the empirical formulae currently available in the scientific literature were applied to predict the lubricant film thickness and a full-film lubrication state or neary-full-film lubrication is predicted with all the testing conditions and lubricants. Par. 5 gives more details.

For linear reciprocating tests, load was kept at the same value as for the corresponding rotating tests, whereas the linear oscillation frequency of the oscillating plate varied in the preliminary phase. Frequency of 3Hz, 2Hz and 1Hz were tried out and it turned out that the higher the oscillation frequency the more uneven is the friction signal. This effect is not totally clear and could be linked to either augmented film thickness dynamics (e.g film thickness fluctuations due to dynamic reactions in response to motion reversal) or stronger vibrations spreading the instrument frame and affecting the very sensitive LVDT sensors output. The former hypothesis is in line with results by Nishikawa and Kaneta [15],[21] for reciprocating EHL point contact. The latter hypothesis is justified by the fact that Anton Paar provides an adapter kit to perform linear reciprocating tests that transforms the standard rotary configurations into the linear motion configuration (Figure 3). It consists of a sliding plate driven by a dedicated mandrel with an eccentric pivot. This adapter kit introduces two main modifications to the instrument mechanical layout: the mass subjected to sinusoidal acceleration is larger, and the driveline suffers some more backlash in couplings between moving parts (e.g. clearance at the eccentric-plate coupling). Mechanical vibrations are likely to grow rapidly with speed as a result, because of stronger shocks across the driveline.

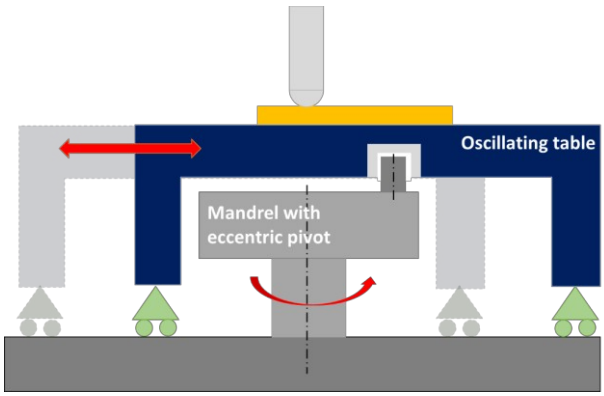

Figure 3. Anton Paar adapter kit to perform linear reciprocating tests.

Figure 4a and 4b shows the comparison among the extreme values: 1Hz (Figur 2b) is the frequency that gives rise to the smoothest friction curve and the best cycle shape (at equal sampling rate, always fixed at 80Hz).

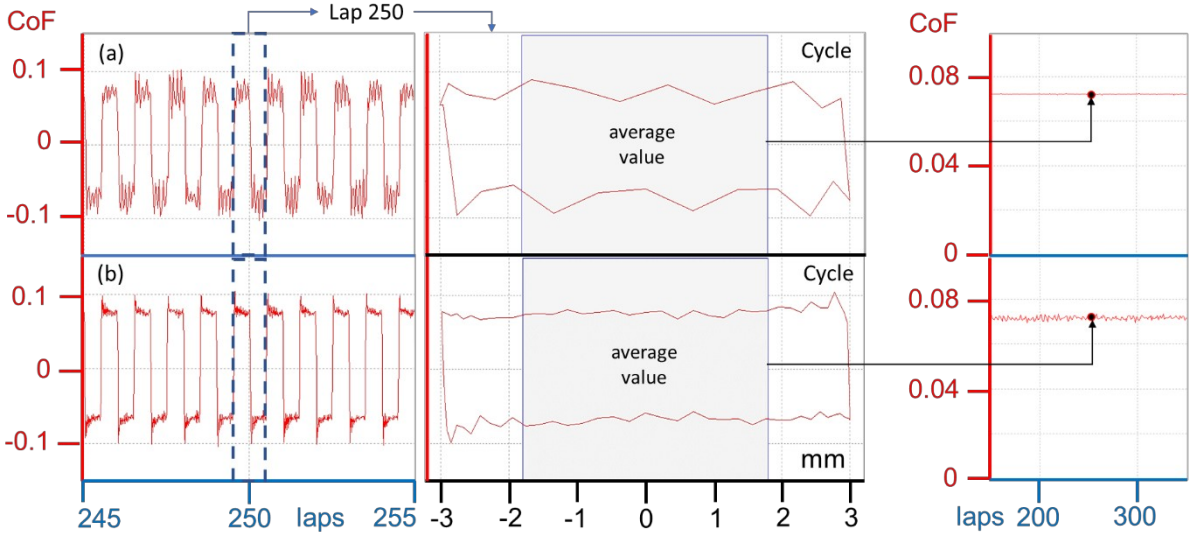

Figure 4. Raw friction curve (on the left), example of cycle shape (in the middle) and equivalent friction curve (on the right) with (a) 3Hz and (b) 1Hz reciprocating sliding frequency.

To allow for comparison with rotating tests, raw friction curves from linear tests (left side of Fig. 4) were analyzed by a cycle-by-cycle averaging technique based on which a single representative average value is extracted from each cycle. The area framed by a blue solid square in Fig. 4 delimits the measuring points of each cycle involved into the averaging process, about 3/5 of a cycle. Only the points placed within the central portion of each cycle were taken into account, because variations of speed are minimum there and the hydrodynamic effect is maximum. In doing so, an equivalent friction curve can be plotted collecting the representative values from each cycle as curve points (see the right-hand side of Fig. 4). This technique allows to represent the output of linear tests through equivalent curves having similar trend as rotary friction curves and comparable average values, so that the former can be compared to the latter. The reader should be able to verify this same graphical technique was exploited in other experimental works dealing with linear reciprocating contacts, like Bai et al.[29].

Table II provides the testing parameters for the 4 measurement conditions selected in the end; each condition was tested separately. Information about the maximum contact pressure is provided in this table for the

individual testing conditions as well. In lubricated point contacts the contact pressure value can be estimated approximately according to the Hertzian elastic contact model. According to Hamrock et al. [33] the fully developed EHL condition, in the sense of the piezoviscous-elastic behavior, usually originates when the maximum contact pressure exceeds 0.5 GPa with common industrial oils. Contact pressure values listed in Table II are inside the above range; no further verifications were carried out, nor possible because of the test rig layout (interferometry was impracticable) and the materials tested (ECR analysis was impracticable).

Table II. Testing conditions

	Load [N]	Spindle Speed [rpm]	Frequency [Hz]	Duration [cycles]	Track radius [mm]	Stroke [1] [mm]	Lubricant quantity [µL]	Contact pressure p_{Hz} (max) [GPa]
MVo (rotating mode)	2	100	-	1000	4 to 7	-	60	0.562
MVo (linear mode)	2	-	1	500	-	6	40	0.562
HVo (rotating mode)	30	150	-	1000	5 to 6	-	100	1.386
HVo (linear mode)	30	-	1	500	-	6	60	1.386

[1] The stroke amplitude is here intended as the segmented length traced by the ball on the disk, i.e one half of the peak-to-peak distance over a cycle.

In this study minor changes in the entrainment speed were accepted and several track radii were sequentially set in the range from 4 to 7mm for the MVo and from 5 to 6mm for the HVo. Rotating and linear reciprocating modes were tested separately as this latter requires a specific module to be installed on Anton Paar tribometers. Every condition was repeated several times with both the tribometers, as specified below in Table III.
Much attention was paid to deeply clean and degrease the entire equipment with chemical pure Acetone and Isopropyl alcohol (IPA) at the end of each test run. Samples and tools were handled with latex gloves and dried with lint-free tissues. Optical microscopy allowed to check the integrity of the glass surface, the absence of wear on the ball and the effective removal of any trace of used lubricant and dust before and after every test run. A temperature and humidity sensor were fitted inside the testing chamber (see Figure 1c) to follow the evolution of the environmental parameters and make sure that each repetition is performed in consistent climatic conditions. The average temperature inside the testing chamber was in the range from 20 to 29°C and moisture content from 30 to 95%. The control of the test rig and data acquisition was both performed with the dedicated Anton Paar InstrumX® Software.
The whole experimental survey took several weeks to be completed and each tribometer has been periodically recalibrated, following the user manual advice.

3. Results

Several repetitions of each testing conditions were carried out: each set covered at least 32 test runs, and many more in most of the cases. Two average tangential force levels were obtained: 0.145N for tests with the MVo and 2.139N for tests with the HVo.

Table III gives an overview on the results corresponding to the conditions listed in Table II with the two tribometers. Figure 5-8 show the output of one friction test belonging to each set of tests listed in Table III. Since each set of tests includes 32 to 58 tests, it is impracticable to present graphically such an amount of data in an aggregated manner. Only one friction curve out of 32 to 58 is then displayed to represent the entire set which it belongs to. Temperature and humidity curves are showed as well, when available as plottable data. . It is here recalled that, in what follows, displayed curves of rotary test are raw data; those of linear reciprocating tests are not raw data. The latter were previously analyzed through a cycle-resolved averaging technique, as already discusses in Sec. 3, in order to depict equivalent friction curves comparable to rotating tests curves.

Table III. Overview of the results of coefficient of friction for each set of repetitions

Instrument	Oil type	Number of samples	Number of repetitions	AAV	St.DAV	ASt.DV	Laboratory
TRB³	MVo (rotating)	3	46	0.0757	0.0014	0.0017	**Anton Paar TriTec laboratory, Corcèlles (CH)**
	MVo (linear)	1	32	0.0702	0.0016	0.0003	
	HVo (rotating)	3	42	0.0758	0.0011	0.0022	
	HVo (linear)	4	37	0.0766	0.0008	0.0002	
TRB	MVo (rotating)	1	38	0.0731	0.0022	0.0035	**Politecnico di Torino, DIMEAS laboratory, Torino (IT)**
	MVo (linear)	2	58	0.0715	0.0006	0.0002	
	HVo (rotating)	3	42	0.0713	0.0011	0.0027	
	HVo (linear)	3	54	0.0767	0.0005	0.0002	

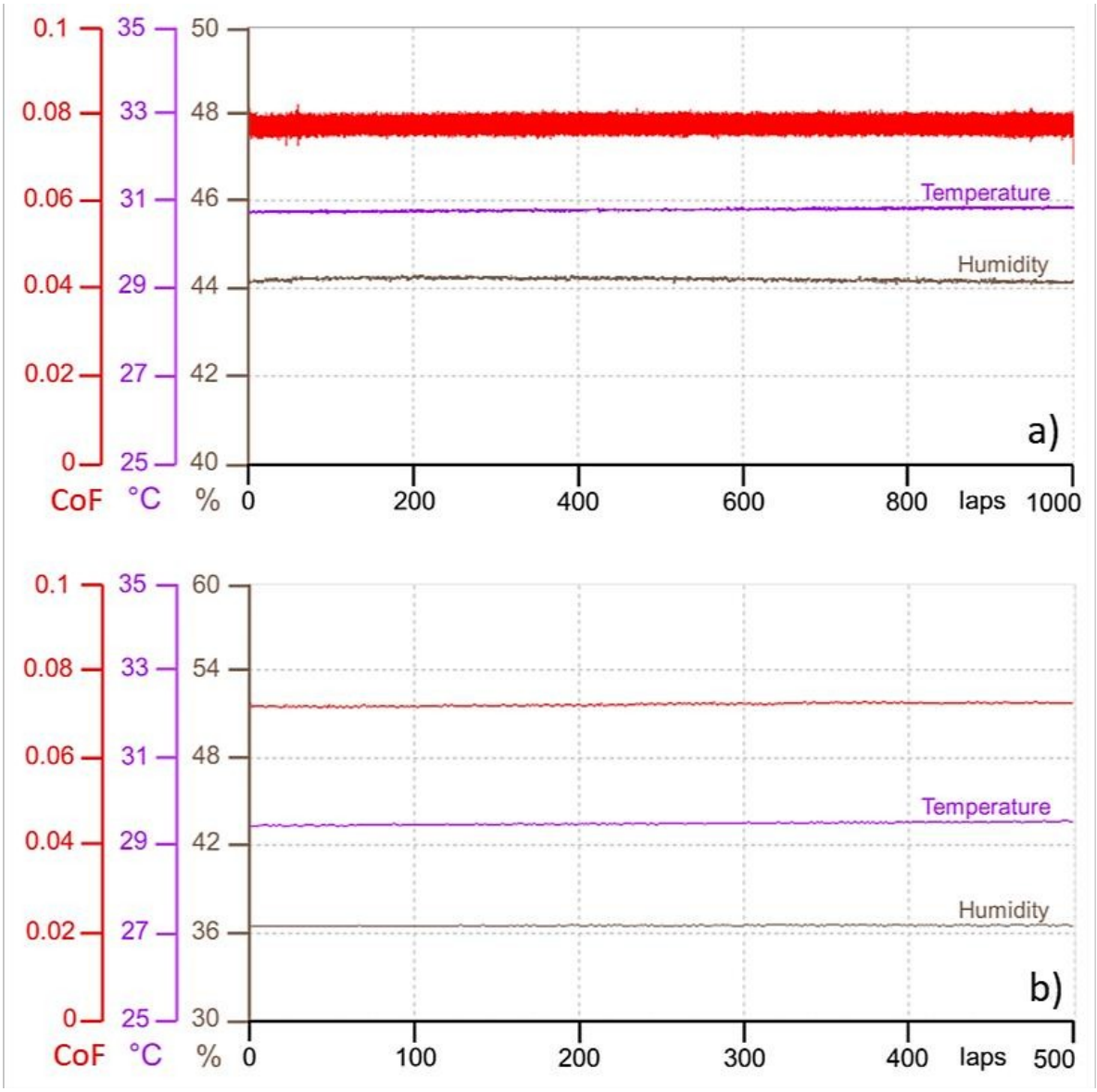

Figure 5. Example of a CoF curve obtained with the TRB[3]and the MVo(2N load) in (a) rotating and (b) linear reciprocating mode.

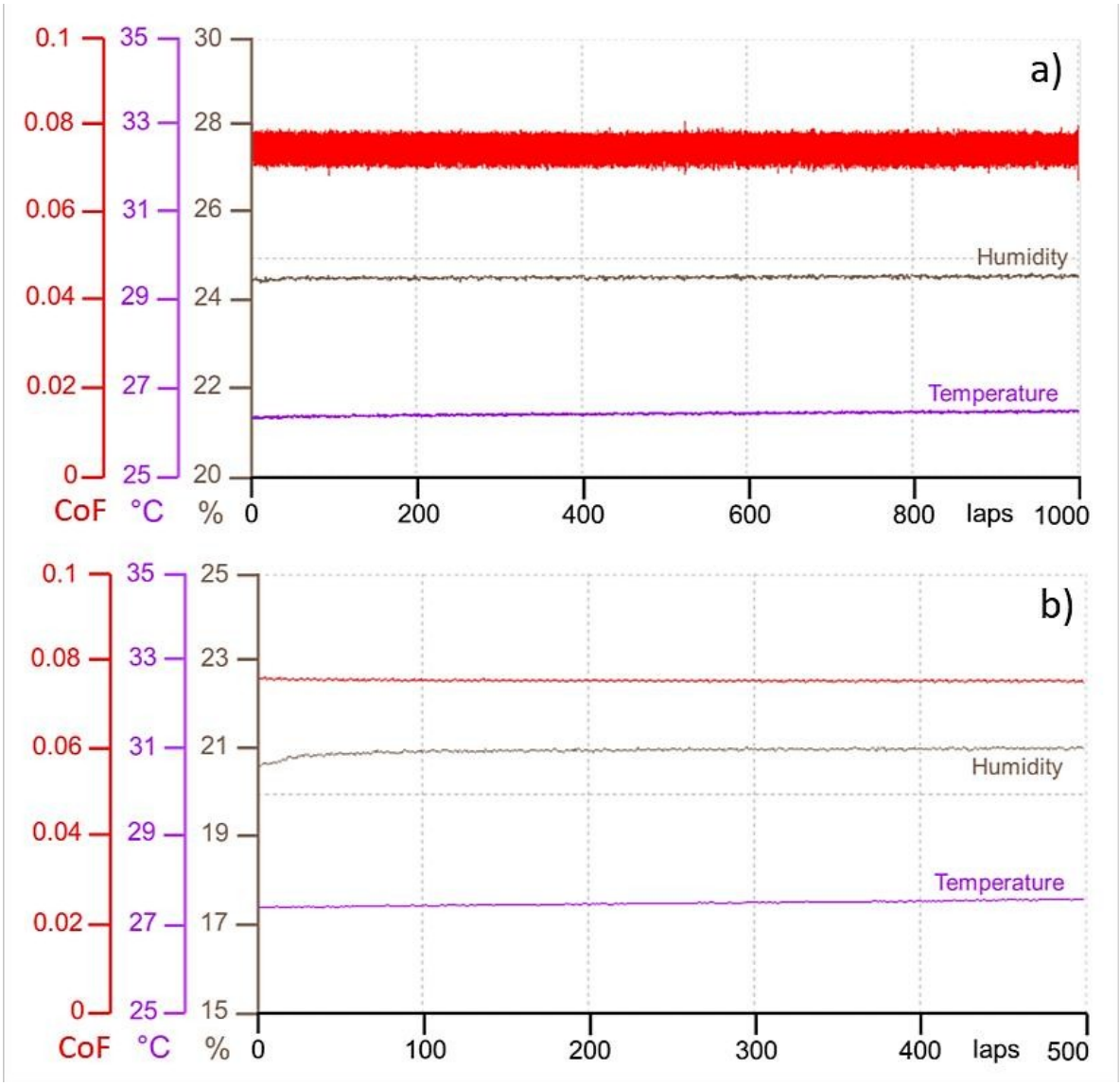

289
290 **Figure 6.** Example of a CoF curve obtained with the TRB[3]and the HVo (30N load) in (a) rotating and (b) linear
291 reciprocating mode.

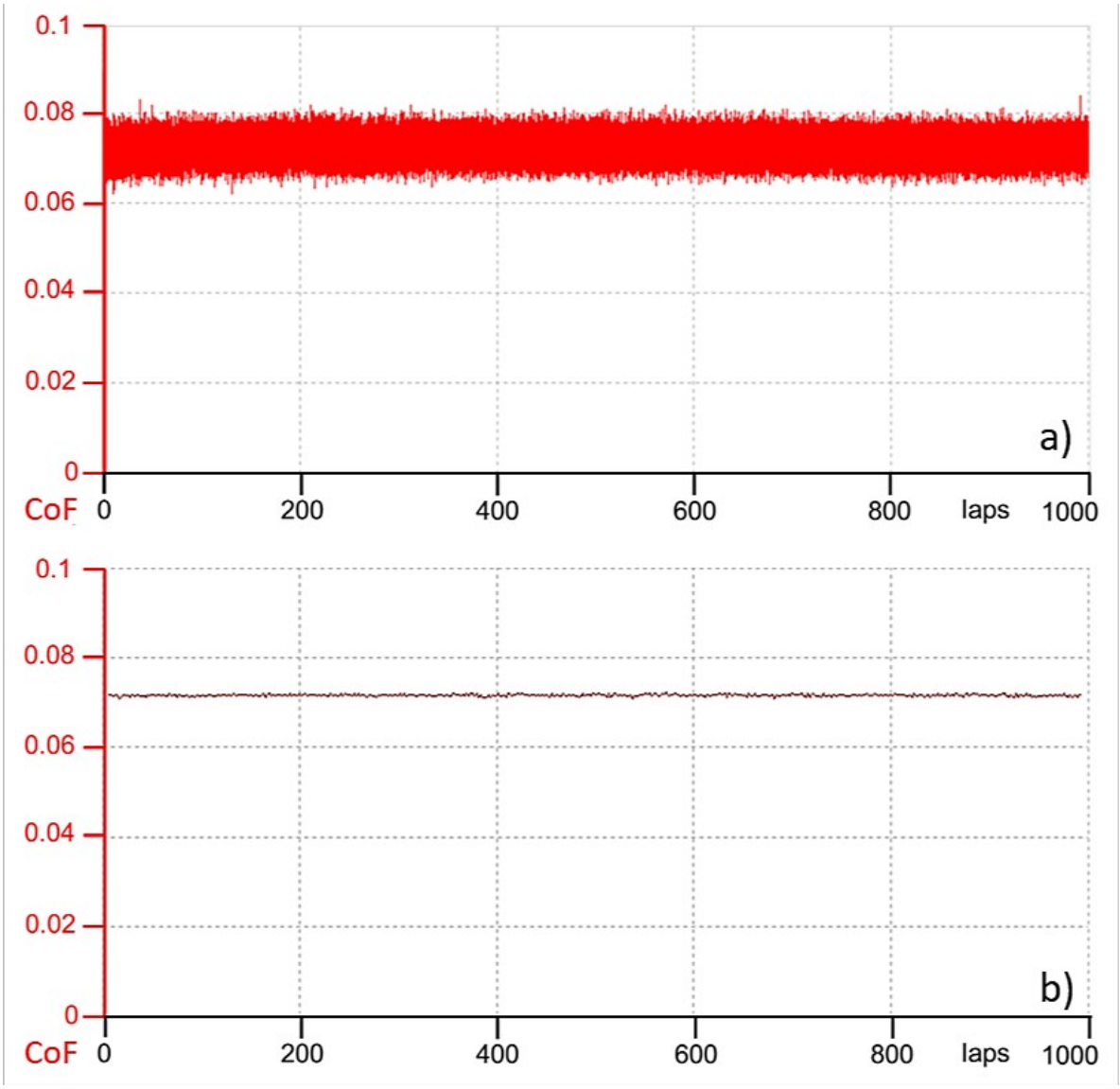

Figure 7. Example of a CoF curve obtained with the TRB and the MVo (2N load) in (a) rotating and (b) linear reciprocating mode.

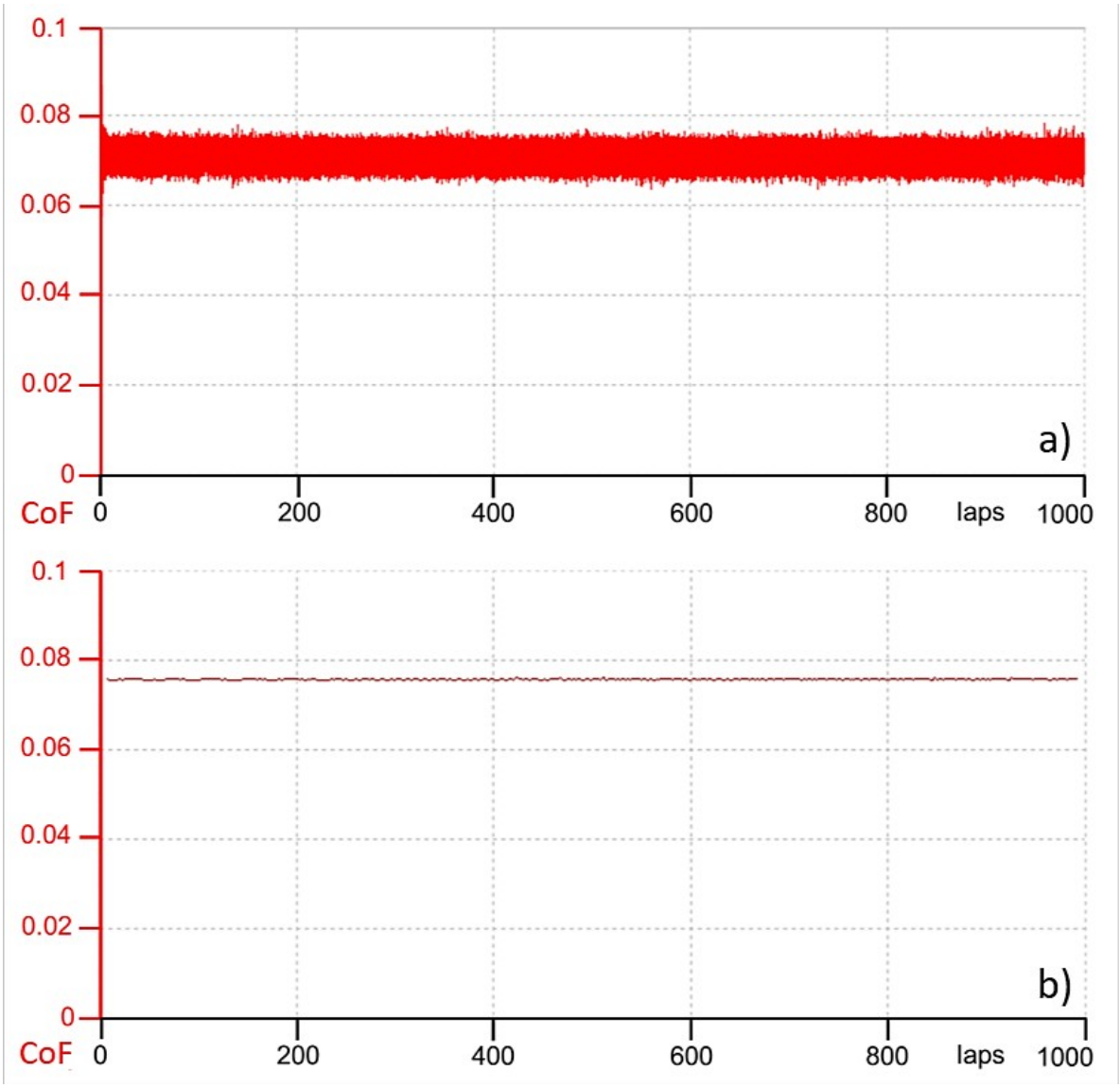

Figure 8. Example of a CoF curve obtained with the TRB and the HVo (30N load) in (a) rotating and (b) linear reciprocating mode.

Fig. 5 to 8 combined with values in Table III prove that all the test runs in all conditions provided exceptionally stable and repeatable results in terms of both friction curves shape and average CoF values. This is also evidence of the fact that the risk of starvation effects (oil loss out of the contact zone) is sufficiently low despite the lack of oil bath. A relevant concern among others is related to centrifugation of the lubricant outside the contact. Grützmacher et al. [27] reported a near no-wear tribological condition in pure sliding ball-on-disc tests at 6mm track radius and 0.08m/s sliding speed with a Castrol PAO30 (30cSt viscosity) oil. They attributed this result to little enough centrifugal forces to have a nearly zero lubricant film shrinking and concluded that higher viscosity results in a less pronounced influence of the centrifugal forces on the lubrication regime. In the present study, friction tests featured much higher viscosity oils and lower rotational speed (thus, centrifugal forces), so that centrifugal effect should be negligible with no impact on the lubricant film build-up and stability at the contact interface. Moreover, Grützmacher et al. used not-additivated oils for which effect of varying adhesive properties on retaining the lubricant in the contact can be neglected. On contrary, commercially fully

formulated oils have additives which strengthen the solid-liquid adhesion properties, thus reducing further the risk of centrifugal oil leakages.

EHL friction tests appeared to be very sensitive to disturbances (shocks and vibrations) coming from the environment, even at low intensity. Example of external disturbances experienced during the experimental campaign are people walking by the machine, noise and vibrations coming from rooms nearby, accidental hits on the table, etc…therefore care should be taken to avoid these kinds of disturbances. The cleanliness of the surfaces played an important role too. While carrying out preliminary tests it also happened that some of these tests produced very unstable friction curves whose mean value and noise were very different than usual ones, despite obvious external disturbances were lacking. This kind of erratic behavior was later proved to be imputable to imperfect cleaning, in particular dust and fibers passing through the thin oil film.

Although ASTM G99 [34] (the sole standard for pin-on-disc tribological tests) recommends using all the data from each set of measurements, including outliers, no test where either the influence of external disturbance or cleanliness issues were obvious has been taken into account in this study, as they are not representative of the instrument working state. The authors of this paper would like to underline that the approach taken in this investigation is not in contrast with the standard anyway. Outliers are values that deviate from the average "by accident", i.e. linked to unavoidable accidental errors associated to the phenomenon under study. In this study, discarded tests are the result of systematic and well identified external causes (anyway impossible to totally overcome). From this perspective, the discarded results are not even attributable to the phenomenon under study, so they are neither outliers.

Such high sensitivity of tests has pros and cons in SHM techniques. A very good detection capability of little damages/problems is expected, by the price of high sensitivity to some healthy changes of operational and environmental conditions too [3].

The box-plots in Figure 9 to 12 show the scattering of the mean values within each set of repetitions presented in Table III. The values of the CoF obtained in this work belong to the range from 0.01 to 0.1 which is very typical for EHL with industrial oils, as confirmed by Stachowiak and Batchelor [35]. Besides, the whole set of average values obtained with both the MVo and the HVo fall inside the sub-range from 0.065 and 0.080. Equivalent friction curves from linear tests feature an apparent lower curve noise and lower scattering because they portray data which have already undergone some processing; for this reason, their scattering is naturally lower.

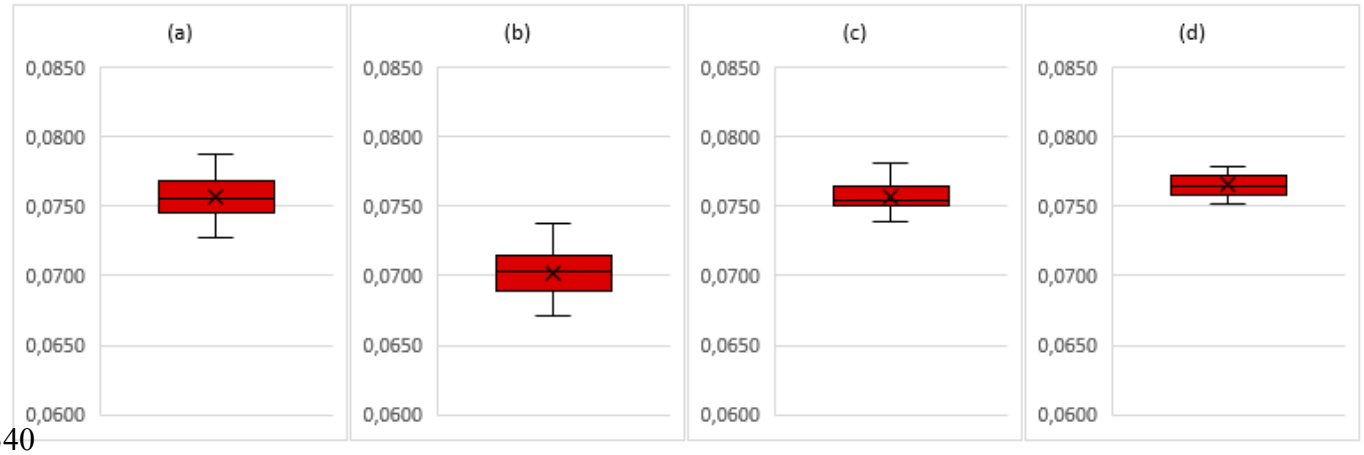

341 **Figure 9.** Box-plots of the mean CoF values for each set of repetitions on the TRB tribometer: (a) MVo rotating
342 tests; (b) MVo linear tests; (c) HVo rotating tests; (d) HVo linear tests.

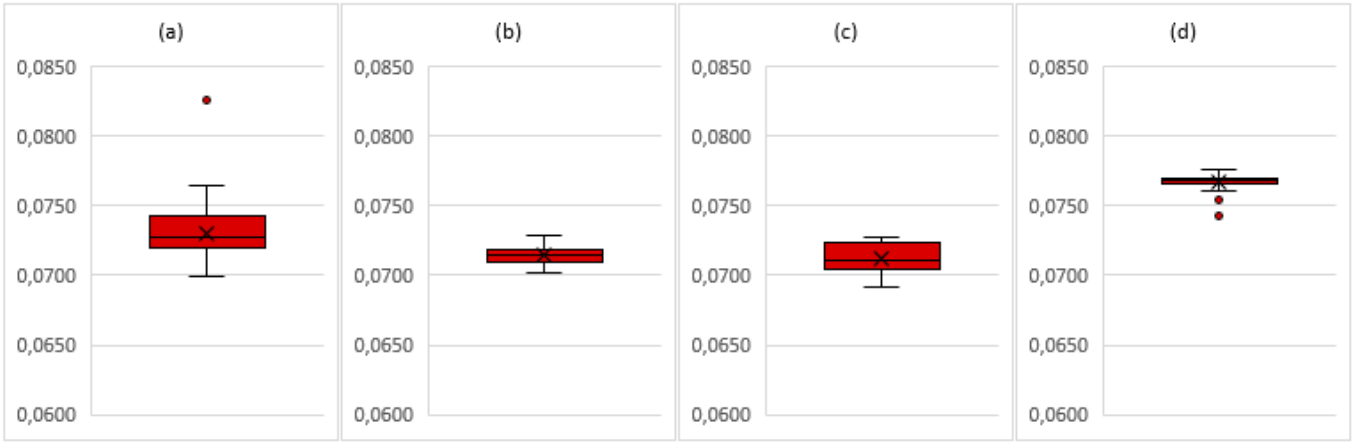

344 **Figure 10.** Box-plots of the mean CoF values for each set of repetitions on the TRB tribometer: (a) MVo rotating
345 tests; (b) MVo linear tests; (c) HVo rotating tests; (d) HVo linear tests.

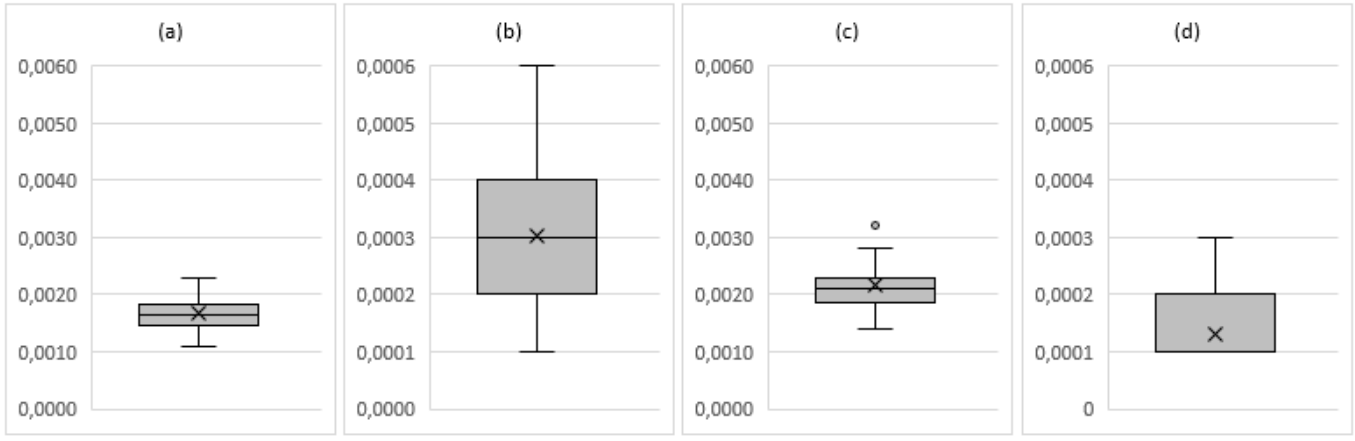

347 **Figure 11.** Box-plots of the CoF standard deviation values for each set of repetitions on the TRB tribometer:
348 (a) MVo rotating tests; (b) MVo linear tests; (c) HVo rotating tests; (d) HVo linear tests.

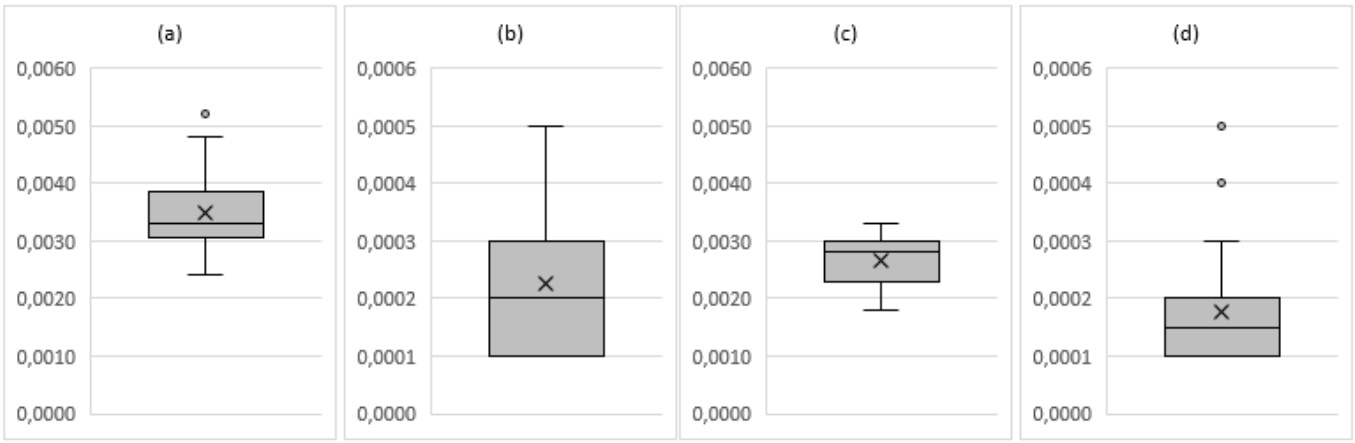

350 **Figure 12.** Box-plots of the CoF standard deviation values for each set of repetitions on the TRB tribometer: (a)
351 MVo rotating tests; (b) MVo linear tests; (c) HVo rotating tests; (d) HVo linear tests.

352 It is commonly known that the environmental state, i.e. temperature and moisture content, influences what
353 happens at the tribological interface.This is true especially in dry contacts, but also lubricated contacts with

little amount of lubricant may be affected . Temperature is a strong influencing parameter, large variations would definitely influence the lubricant rheological behaviour performance and thus friction measurements. Conversely, the moisture content variations could turn out to be less important. The main concern about humidity is the risk that water droplets condensate on the oil surface; if the little amount of lubricant is not able to completely insulate the contact region from the environment, the lubricant might become a water-oil mixture and load bearing capacity might be affected. In order to be sure that humidity has no influence on friction curves despite the little amount of oil, some additional sets of tests were carried out into an environment close to the dewpoint. These comparative tests (whose results are omitted) revealed that the contact zone is effectively insulated from the environment and procedures apply regardless of the ambient humidity.

The effect of temperature was not directly addressed in this study because the instruments were operated in thermally stable environments. As a general rule, temperature variations should be kept within a well-defined narrow range for the sake of reference measurements. However, scientific instruments like tribometers are usually operated in laboratory rooms where temperature is controlled well enough (20°C to 30°C typically) to neglect temperature effects.

4. Discussion

4.1. Statistical analysis of results

For the sake of statistical analysis, each test has been accounted for through two statistical parameters which describe the friction curve appearance: the average ($\bar{\bar{C}oF}$) and standard deviation ($CoF_{St.Dev.}$) of the experimental CoF points of test. The overall statistics has been compiled by collecting these two parameters from each test to calculate three representative quantities for each series of tests:

- The average of the test average values $\bar{\bar{C}oF}$ (herein referred to as AAV);
- The standard deviation of the test average values $\bar{\bar{C}oF}$ (herein referred to as St.DAV);
- The average of the test standard deviation values $CoF_{St.Dev.}$ (herein referred to as ASt.DV).

Section “Discussion” will return to these statistical quantities to reveal the tribometer-to-tribometer variability and the test-to-test variability for each condition.

Based on values listed in Table III, two types of variability of the results within each set of repetitions are discussed below: tribometer-to-tribometer variability and test-to-test variability.

Details on the tribometer-to-tribometer variability of the CoF mean value can be deducted comparing the AAVs in similar conditions by different instruments. Percentage-point differences are listed in Table IV and it is quite evident that repeatability on different instruments is very good.

Table IV. Tribometer-to-tribometer variability

Representative quantity	MVo – rotating	MVo – linear	HVo – rotating	HVo – linear
AAV_{TRB} - AAV_{TRB3} [%]	3,5%	2%	6%	0.2%

The St.DAV has to be taken into account to evaluate the test-to-test variability on the same tribometer in equal testing condition, see Table V. Values of the St.DAVs ranging from 0.65% to 3% of the corresponding AAVs point out that the scattering is low for each testing condition, even though more than one sample are used

Table V. Test-to-test variability

Tribometer	Representative quantity	MVo – rotating	MVo – linear	HVo – rotating	HVo – linear
TRB	St.DAV / AAV [%]	1.85%	2.23%	1.45%	1.04%
TRB[3]		3.00%	0.84%	1.54%	0.65%

. Much of this scattering is believed related to the gluing of the glass disco onto the stub and to the position change of the two counterweights necessary to equilibrate the arm own weight. Since the entire experimental campaign was carried out over several weeks, the counterweights position changed repeatedly, and a slightly different position of the counterweights means a slightly different effective load applied on the contact. The CoF is very low, thus even minimal variations are found to affect somewhat the test mean value. For the same reason, a contribution coming from the tolerance of the arm balancing must be accounted for the difference between the AAV obtained with various instruments.

The ASt.DV measures the average friction curves noise over a series of tests in same conditions. Table III shows that a similar noise (i.e. the "thickness" of the friction curve itself) characterizes the curves measured in the same test condition by the same instrument. A tiny noise variability may appear if the same test is repeated by different instruments (tribometer-to-tribometer variability) and may also appear using different samples, but measurements remain always consistent with one another. The thickness of friction curves seems to be an instrument own characteristic, but further verification on many more tribometers will be necessary to validate this conclusion. Linear tests have an ASt.DV that is one order of magnitude smaller than the corresponding value of rotating tests with the same oil. Such a discrepancy is nevertheless more apparent than real: being linear tests analyzed with a cycle-by-cycle averaging technique their ASt.DV suffer, in a way, double averaging.

4.2. Reference testing procedure

It becomes clear that each test condition owns a characteristic mean value and, to some extent, a characteristic standard deviation value of the friction coefficient; both disclose little to no affecteion by the instrument used to run the test. This value is herein referred to as the 'Characteristic AAV' and calculated by further averaging the corresponding AAVs by the two instruments (see Table III). The characteristic AAV is reported in Table VI along with the other global statistical quantities calculated similarly.

Table VI. Global values

Lubricant	**Test configuration**	**Characteristic AAV**	**Global St.DAV**	**Global ASt.DV**
MVo (2N)	Rotating	0.0744	0.0018	0.0026
	Linear reciprocating	0.0708	0.0011	0.0003
HVo (30N)	Rotating	0.0735	0.0011	0.0024
	Linear reciprocating	0.0767	0.0006	0.0002

On the basis of these data, reference ranges of acceptability for the CoF are proposed for each testing condition and the corresponding limiting values are displayed in Table VII. Reference ranges of acceptability involve both the CoF test average and its test standard deviation. These ranges of acceptability for the CoF average are determined as follows:

$$\begin{cases} (Characteristic\ AAV + 3 \cdot Global\ St.\ DAV) < \bar{\bar{C}}oF < (Characteristic\ AAV - 3 \cdot Global\ St.\ DAV) \\ CoF_{St.Dev.} < Max(St.\ Dev) \end{cases}$$

where the Max(St.Dev.) is equal to the maximum standard deviation value recorded during each series of tests in this study.

Any user disposes of two parameters to assess the proper functioning of its own tribometer: the average CoF value of the reference test must remain into the prescribed range and the standard deviation value of the same test should not exceed the prescribed value.

These ranges of acceptability are proposed as a yardstick through which assessing whether a tribometer is properly working with enough confidence. Ranges of acceptability are necessary to account for imperfect reproducibility of test conditions and unavoidable production differences among the instruments, as already addressed above in Par. 4.1.Whenever one of the two parameters do not meet the requirements, no further specific instructions are provided by such procedure in the present release anyway, except that something is going wrong with the tribometer. Features extraction from the monitoring parameter signal would be necessary indeed to obtain complete information on potential damages of the instrument [3]; e.g. through a case study based on known damages/malfunctions one could provide the atlas of correlations between the occurrence of some damages/malfunctions and the output of the reference test. This further step has not been included yet in this work. Nonetheless, this procedure is already able to perform a useful technical diagnosis. If the average value is out of range and the test is performed correctly (no effect of contamination or dust, etc...) then a problem of calibration of the instrument could be there, or a sensor failure or even the arm manufacturing fault (the measuring arm stiffness is calibrated). On contrary, if the standard deviation is out of range, it could suggest that abnormal vibrations due to either the spindle bearings, or the electric motor, or some other poorly fixed component is arising; or even that an electrical disturbance problem due to electronic cards may distort the measured CoF signal.

Table VII. Ranges of acceptability

Lubricant	**Test configuration**	**Acceptable range for the CoF average value**		**Acceptable CoF standard deviation**	
		Lower bound	**Upper bound**	**Maximum value**	
MVo	Rotating	0.069	0.080	TRB[3]:	0.0026
				TRB:	0.0052
	Linear reciprocating	0.068	0.074	TRB[3]:	0.0006
				TRB:	0.0005
HVo	Rotating	0.070	0.077	TRB[3]:	0.0032
				TRB:	0.0033
		0.075	0.079	TRB[3]:	0.0004

	Linear reciprocating	TRB: 0.0005

5 Checking the EHL contact condition

The pin-on-disk set-up does not allow any direct film thickness measurements. In this specific case, interferometric measurements were impracticable because of the test rig layout and ECR analysis was impracticable because the tested materials are electrical insulating. However, there exist indirect evidence suggesting that the ball and the sample were separated by a continuous film of lubricant in all the tested conditions. Notably, no signs of wear on the ball and sample were visible under the optical microscope, and friction curves were very regular and smooth with a low CoF value.

The precise determination of the lubrication regime is not the primary objective of this paper. The friction coefficient is the star in this paper indeed, not the lubricant film thickness, and its repeatability is the core feature of the proposed test condition. With that in mind this section has been introduced just in support of the above experimental evidence, so as to strengthen the plausibility of the no-wear regime (as microscope inspection suggests) and focus the correlation between lack of visible wear and CoF repeatability in tribological testing.

Some of the currently available empirical formulae to predict the lubricant film thickness were applied blindly, according to the task they have been developed for. The film thickness and the corresponding value of the roughness factor Λ[2] (or lambda ratio) is computed for the tests in rotating mode only. The lambda ratio has no unified definition: someone defines it as the ratio of the central (or average) film thickness to the composite roughness, like Tallian et al. [36] and Poon et al. [37], others refer to minimum film thickness to be more conservative, like Stachowiack et al. [33] and Hamrock et al. [35], others do even make it clear, for instance Bair and Winer [38]. For the sake of precaution, the minimum film thickness at the exit region of the contact is taken into account here.

The output of three empirical formulae are compared: the popular equation by Hamrock and Dowson [6], one model developed specifically for EHD sliding contacts by Wilson and Shew [39] and the general equation proposed by Masjedi and Khonsari [40]. Strictly speaking the film thickness theory by Hamrock and Dowson was originally developed for nominal pure rolling contacts; though some authors in the scientific literature state that it may also apply to slide-roll conditions [41],[42]. Wheeler et al. [42] represented on a M-L plane the validity range of several empirical equations by a number of authors, M' and 'L' being the Moes' parameters [43]. According to this map, Masjedi and Khonsari formula better describes the testing conditions explored in this study. The corresponding Moes parameters are L=9.47, M=1219.9 for the MVo and L=18.7, M=2377.2 for the HVo tests. The reader can verify that these values identify two points laying into the Masjedi and Khonsari equation domain into the diagram reported in [42].

Table VIII summarizes the values of the physical properties and geometrical parameters having a role in the film thickness equations. Non-dimensional parameters 'U', 'W' and 'G' are computed according to Hamrock and Dowson and 'C' is the thermal-sliding correction factor introduced by Wilson and Shew [39]. The 'C'

[2] The roughness factor is classically defined as: $\Lambda = h_{min}/\sqrt{R_{q,1}^2 + R_{q,2}^2}$ where h_{min} is the minimum lubricant film thickness and $R_{q,1}$, $R_{q,2}$ are the root-mean-square values of the mating surfaces roughness.

factor takes into account the inlet shear heating effect and is basically used as pre-multiplying factor for the Hamrock and Dowson equation. The 'C' factor is function of the SRR and the thermal loading parameter 'L_t' which takes into account the temperature-viscosity effect and the thermal conductivity of the lubricant [39]. Figure 13 represents the Hamrock-Dowson's chart of the EHD operating conditions for lubricated rolling-sliding point contacts [33]. It ensures that the lubricated interface is subjected to the piezoviscous-elastic behavior with both the MVo and the HVo, which is the range of applicability for the above formulae. G_V and G_E are the dimensionless Hamrock's viscosity and elasticity parameters.

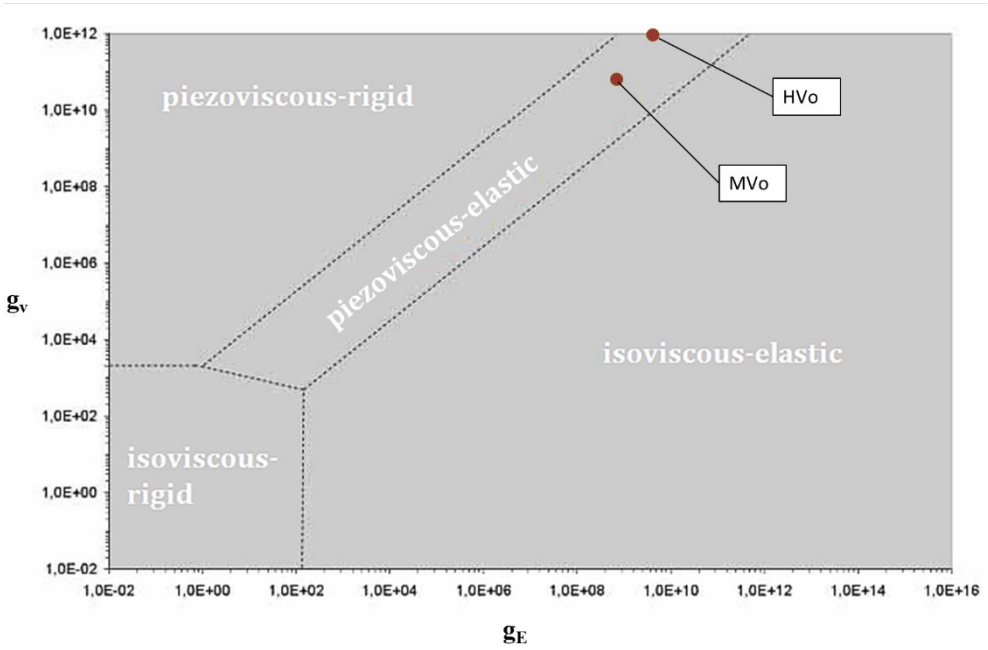

Figure 13. Hamrock-Dowson's chart of EHD operating conditions highlighting the points corresponding to the tests with the MVo and HVo.

Table VIII. Summary of the physical and geometrical parameters

Common parameters		**Specific parameters**	**MVo**		**HVo**	
			Rotating	Linear	Rotating	Linear
R_d [m]	0.003	**v_d [m/s]**	0.0628	0.0189	0.0942	
R_b [m]	∞	**v_b [m/s]**	0.0000	0.0000	0.0000	0.0000
k [1]	1	**$\bar{U}$ [m/s]** [1]	0.0314	0.0094	0.0471	
R' [m] [1]	0.0015	**F_N [N]**	2	2	30	30
E' [GPa] [1]	129	**η_0 [cP]**	105.2		621.1	
SRR	2	**α [GPa^{-1}]**	30.5		34.8	
		α_T [K^{-1}] [2]	3.66		2.74	
		h [Wm^{-1} K^{-1}] [3]	0.18		0.31	

[1] Entrainment speed calculated according to Hamrock et al. [44].

[2] Here assumed equal to the "ASTM slope" [34] form Walther formula.

[3] Thermal conductivity for the HVo has been calculated according to the formula proposed by Larsson and Andersson [45] for PAO. Being the chemical composition of the MVo confidential, a typical value for light oils has been taken into account for the calculations.

Table IX lists the forecast provided by each equation. Since sliding speed was handled as an almost free parameter, which varies in the narrow range corresponding to the track radius variations defined in Table II, the forecasts in Table IX were calculated for the mid-range linear speed, i.e. at 5.5mm track radius.

Table IX. Predicted values of the roughness factor (rotating mode only)

Oil Type	Equation	p_{Hz} (max) [GPa]	U	W	G	C	L_t	Calculated h_{min} [nm]	Λ
MVo	Hamrock and Dowson [6]	0.564	$1.72 \cdot 10^{-11}$	$6.92 \cdot 10^{-6}$	$3.91 \cdot 10^{3}$	-	-	17.6	1.22
	Wilson and Shew [39]					0.931	0.002	10.7	0.75
	Masjedi and Khonsari [40]					-	-	17.3	1.20
HVo	Hamrock and Dowson [6]	1.391	$1.52 \cdot 10^{-10}$	$1.04 \cdot 10^{-4}$	$4.47 \cdot 10^{3}$	-	-	68.0	4.71
	Wilson and Shew [39]					0.813	0.012	43.3	3.00
	Masjedi and Khonsari [40]					-	-	69.8	4.84

Hamrock and Dowson equation and Masjedi and Khonsari equation give similar outputs. Both predict Λ close to unity for the MVo and greater than 4 for the HVo. By the way, the Hamrock and Dowson formula for minimum film thickness is known to be conservative as predicts film thickness slightly lower than measured [33]. Wilson and Shew's formula is the worst-case scenario as it considers the diffused shear thinning effect due to sliding. This model allows for shear stress to produce heat into the nanometric lubricant film; heat is responsible for the loss of viscosity and load-bearing capacity with reduces the supporting lubricating film, as a consequence. According to this model, if L_t is lower than 0.1 then thermal effects are usually said to be negligible [39] and the lubricant behaviour should not differ very much from that in pure rolling conditions. Nonetheless, this approach likely reveals too conservative for the scenario under consideration. In this work the spindle speed was kept as low as possible primarily to avoid any contribution from the tribometer dynamics. This contributed also to keeping L_t at low values, i.e. thermal effects should be limited, especially when viscosity is low. Despite the L_t factor takes a value much lower than 0.1 a non-negligible 10% to 20% reduction of the Lambda ration appears in all the cases (see 'C' factor values in Table IX). Identification of alfa and k in Lt may have played a role since no experimental values are available for these quantities (see Table VIII).
In the opinion of the authors, however, although a 10% or 20% is not a negligible difference, the the lubrication regime foreseen by Wilson and Shew's formula does not differ significantly compared to the other formula.
The predicted conditions for the MVo are always a limiting full-film lubrication (or an extremely smooth mixed lubrication) with Λ about 1, no matter what the equation used; similarly, complete full film lubrication is always expected with the HVo since Λ is always equal or greater than 3, no matter what the equation used.
.

The lambda ratio is a very easy-to-use parameter to correlate the film thickness to lubrication regimes and friction. Its use among engineers and researchers is persistent, evidence that a vast need for such a simple tool there exists for estimating the state of lubrication in industrial problems such as in machine components design. However, it has many limitations and some authors in the scientific literature have agreed over the years that establishing a relation between the film thickness and the initial (nominal) surface roughness is not sufficient to foreseen precisely the lubrication state and the related level of friction [46], [47], [48]. In the past years various authors have plotted experimental Stribeck curves (or Stribeck-like curves) against the roughness factor proposing a number of threshold values for Λ setting the onset of mixed and full-film lubrication; among the others it is worth to cite Tallian et al. [36], Poon et al. [37] and Bair and Winer [38]. This is mainly due to the fact that roughness related effects in EHL problems are scale dependent and operating conditions dependent (see [48], [46] and [35]), meaning that limiting values of Λ, if any, are themselves virtually function of roughness, lubricant properties and operating conditions.

For this reason, setting Λ limiting values of general validity is hardly feasible. Generally speaking, mixed lubrication is observed when $1<\Lambda<5$ and full-film EHL when $\Lambda>3$ [33] (the reader should notice that the ranges overlap). In the range $1<\Lambda<3$ mixed lubrication often comes down to some glazing of the surface; asperities flatten out either elastically or plastically under extreme pressure and effective body separation exists even if estimated lubricating quality still suggested vast contact interference [16] (micro-EHL' occurs [35]). This explains why a lot of machine elements operate with little apparent damages close to $\Lambda=1$ where surface distresses should prevail [35]. This same motivation could explain why no wear appears in tests with the MVo despite the estimated lubricant film is of the same order of magnitude of roughness.

Moreover, E' in Table VIII accounts for the Young modulus of ruby (sphere) and bulk glass (disc) only. Any contribution to the local deformation coming from the glue beneath the disc has been overlooked; glues have elastic moduli of few GPa. Being the glass disk very thin, the equivalent surface compliance of the flat counter body could be higher than what is considered in calculations. Lastly, the roughness factor has been calculated with respect to the minimum film thickness value, which is conservative. The minimum film thickness characterizes the two lateral necking structures in the contact outlet region, representing a very tiny portion of the whole contact though. Even though rubbing of the bodies were assumed, asperities interaction would be restricted to this tiny portion of the contact. Most of the contact is supported in the central flat region in fact, where lubricant thickness is expected to be larger (1 to 3 times larger than minimum film thickness, at least under isothermal Newtonian lubrication conditions [49]).

To the best of the authors knowledge, no empirical equations have been developed to predict the film thickness of sliding EHD point contacts in linear reciprocating mode. Two attempts were made by Petrusevitch et al. [50] and Hook [51], but for nominal line contact only (e.g. cylinder-cylinder contact). Previsions from formulae for stationary conditions cannot be fully trusted as they are not able to properly describe the interface condition along the whole stroke. They might roughly represent what happens at the stroke mid-point, where the kinematic approaches stationary conditions, but they would predict a null film thickness at both the stroke ends where speed is nominally zero. According to Nishikawa et al. [21] fluid-dynamic effects assure non-null film thickness even under motion direction reversal.

6. Conclusions

In this paper two industrial reference testing conditions were developed on two Anton Paar pin-on-disc tribometers for two testing mode: unidirectional rotating and linear reciprocating mode. Two commercial oils were compared, a middle viscosity oil (MVo) and a high viscosity oil (HVo). A special lubricated contact with no lubricant bath was tested where a little amount of lubricating oil was added on the top of the sample before each test. Despite the absence of any oil bath, the lubricant surface tension has proven high enough to retain the oil in the contact area, preventing the transition from full-film lubrication to starved lubrication with sufficient confidence. This set-up was selected as it perfectly meets some key features required for reference tests suitable to industrial applications: it minimizes cleaning issues and the related waste of time; it lowers the risk of lubricant contamination and avoids material waste. The result is a process easy to prepare and carry out, cheap and potentially fit for the application on any tribometer whatsoever.

As to the oil quality, the HVo look a priori the best choice in terms of performance within the scope of this application, as its higher pressure-viscosity coefficient ensures a stronger supporting effect and larger calculated lubricant film. Available formulae for film thickness allowed indeed to estimate the lubrication regime for the testing conditions in rotating mode to a first approximation; based on available data, full-film lubrication is to be expected for the HVo and a very gentle mixed lubrication for the MVo where separation of the rubbing bodies still exists. Nevertheless, the use of the MVo has still many advantages. Since perfect cleaning is of paramount importance, the degreasing procedure after each test is particularly laborious even if small amounts of the HVo are used. Acetone and common gasoline, which are normally aggressive enough to dissolve the MVo, usually fail and specific strong spray solvents must be used in the interest of saving time. Therefore, the MVo is still preferable for verification tests at low contact load, due to the ease of applying and removing the lubricant, keeping the equipment clean and, consequently, lessening the environmental impact.

All the test runs provided exceptionally stable and repeatable results, as discussed earlier in this paper, but an extensive investigation on a number of tribometers is necessary in the future anyway to understand to what extent these values are actually reliable. Moreover, all these significant results were attained with no strict requirements either in terms of speed, which is the most influencing parameter over the EHL regimes, or in terms of geometrical repeatability of samples. Therefore, the proposed method may apply to the technical diagnosis of tribometers by letting users make, at least, a preliminary assessment on the proper functioning of the instrument itself.

This paper is intended as the first step of a more comprehensive investigation which would need many more pin-on-disk tribometers of a number of manufacturers. A case study on the effectiveness of this procedure in highlighting an existing malfunction would be meaningful, e.g. by reproducing known typical troubles and malfunctions then recording the output of the same reference test.

If these further observations would disclose promising results, the outlined procedures could be proposed to become part of an international standard and adopted by those industrial laboratories which require regular examinations of their tribometers. It may be also an effective verification method for inter-laboratory cross studies, before which a common sample should be tested to make sure the instruments all provide consistent measurements.

Appendix A – Instruments Specifications

Instruments specifications are presented in Table A1 in compliance with manufacturers technical specifications.

Table A1. Technical specification of the two Anton Paar Tribometers

Machine specifications	TRB^3	TRB
Normal load (dead weight/s)	0.25N to 60 N	0.25 to 60 N
Friction force	up to 20 N	up to 20 N
Friction force resolution	0.06 mN	0.06 mN
Rotation speed	0.2 - 2000 rpm	0.3 – 1500 rpm
Rotation speed resolution	0.0001 rpm	0.0001 rpm
Linear frequency	0.01 - 10 Hz	0.01 - 10 Hz
Linear stroke	up to 60 mm	up to 60 mm
Linear stroke resolution	2 mm	2 mm
Sample diameter	up to Ø 56 mm	up to Ø 60 mm
Radial position (radius)	up to 40 mm	up to 40 mm
Radial position resolution	0.05 mm	0.05 mm
Angular position resolution	0.1°	0.1°
Relative Humidity	0% to 99% (integrated)	15% to 99% (external)
Relative humidity resolution	0.01%	0.8%
Temperature	-45° to 125°C (integrated)	-100° to 200°C (external)
Temperature sensor resolution	0.015 °C	0.1 °C

Appendix B – Lubricants technical data

Table B1 provides the data about viscosity and other physical properties for the two lubricating oils used in this experimental work. Data correspond to certified values provided in technical sheets by certified laboratory.

Table B1. Physical properties of lubricating oils

OILS	Property	Test method	Value
Middle Viscosity oil (MVo)	Density @15 °C [kg/dm^3]	ASTM D1480	0.861-0.862
	Viscosity [cSt] @40°C	ASTM D445	57

	Viscosity [cSt] @100°C		7.6
	Viscosity Index	ASTM D2270	101
	Flash Point [°C]	ASTM D92	225
	Pour Point [°C]	ASTM D97	-15
High Viscosity oil (HVo)	Density @25 °C [kg/dm^3]	ASTM D1480	0.844
	Density @40 °C [kg/dm^3]		0.835
	Density @100 °C [kg/dm^3]		0.799
	Viscosity [cSt] @25°C	ASTM D2162	1008.0
	Viscosity [cSt] @40°C		421.0
	Viscosity [cSt] @100°C		41.4
	Viscosity Index	ASTM D2270	123
	Flash Point [°C]	ASTM D92	>93

609

610 **Appendix C – Atlas of rejected tests**

611 Table C1 collects some examples of discarded tests in unidirectional rotating mode related to identified causes.

612 Table C2 is the corresponding table for linear reciprocating tests.

613 **Table C1.** Atlas of rejected tests in unidirectional rotating mode tests

Category	Curve appearance	Possible disturbances sources
Better to discard	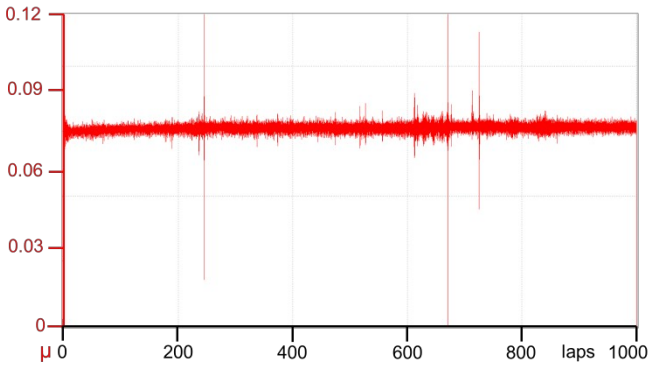	Minor vibration impact e.g. slight touch on the monitor or table

Better to discard	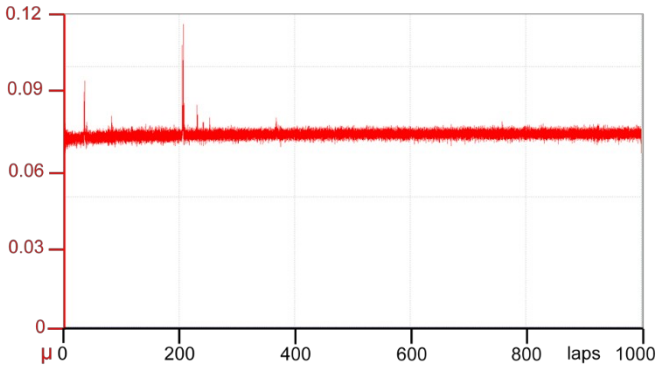	Small fibers in the oil. Dust on sample surface or in the oil;
Better to discard	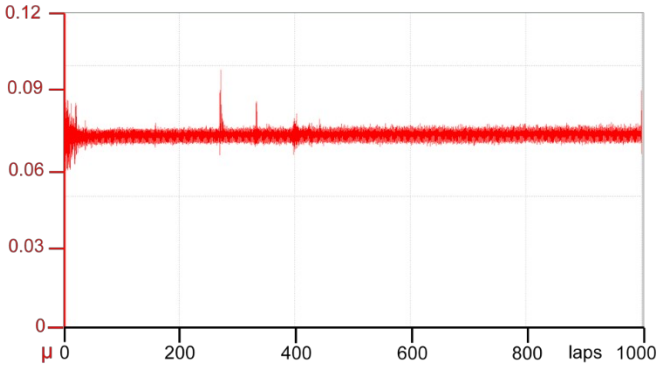	Small fibers in the oil. Dust on sample surface or in the oil;
Discard	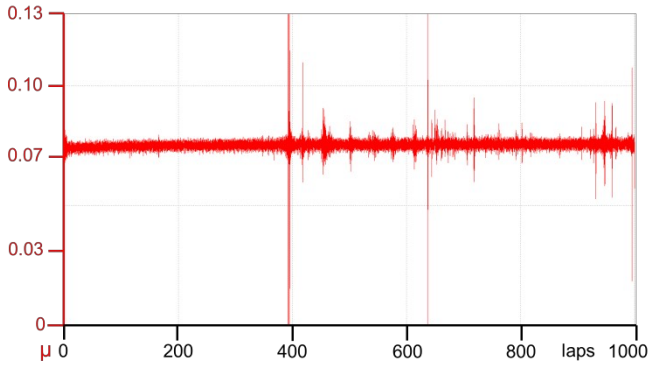	Major vibration impact e.g. passage of a heavy forklift nearby the instrument
Discard	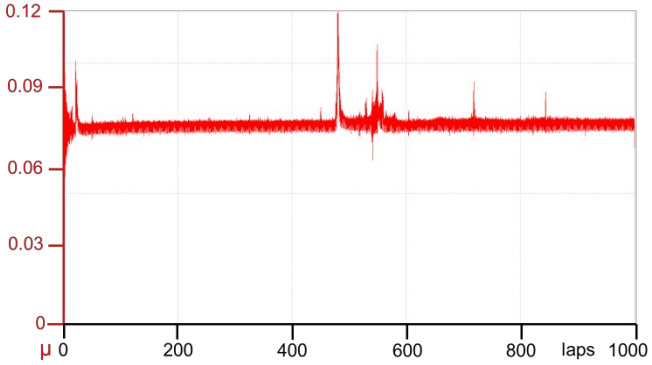	Trace of oil left on the surfaces. Large fibers laid on the surfaces;

	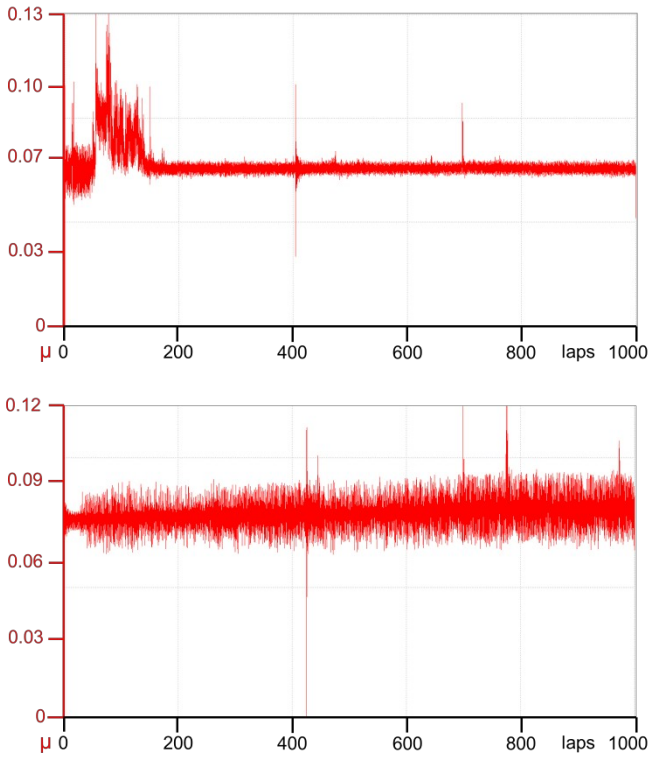	
Discard	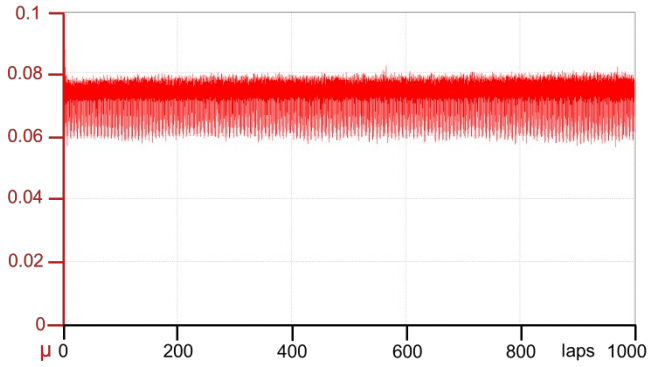	Severe damage or scratch on the sample surface

Table C1. Atlas of rejected tests in linear reciprocating mode tests.

Category	Curve appearance	Possible disturbance sources
Better to discard	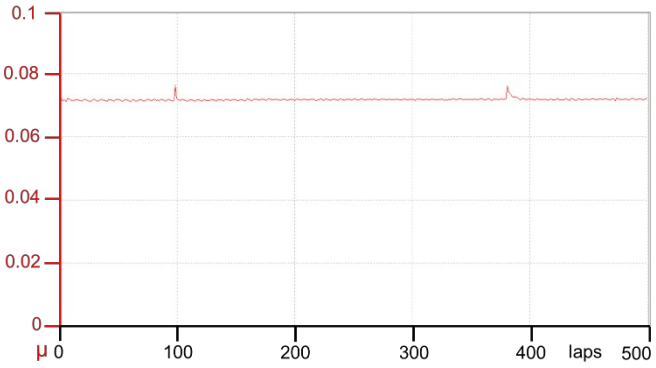	Small fibers in the oil. Dust on sample surface or in the oil

Discard	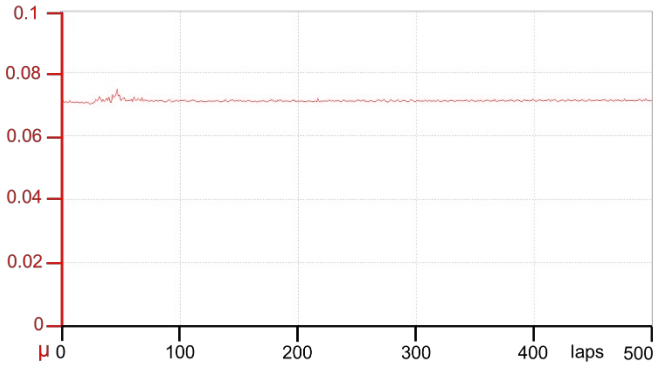	Small fibers in the oil. Dust on the sample surface or in the oil
Discard	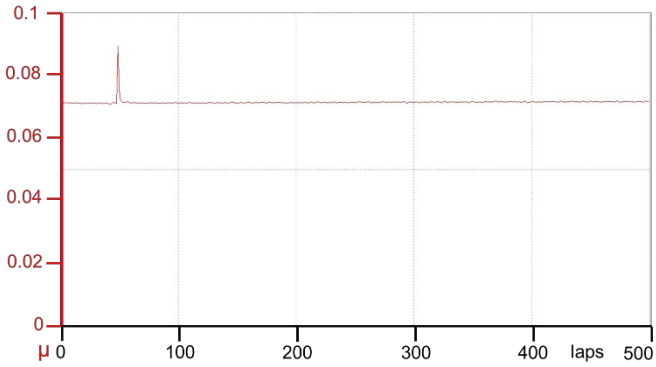	
Discard	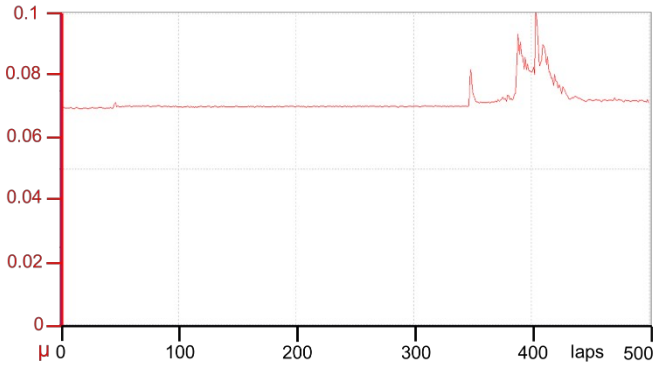	Sample imperfectly cleaned. Large fibers passing through the contact region.

Acknowledgments

The authors would like to acknowledge Anton Paar Italia for the its support in the development of this study.

References

[1] P.J. Blau, Friction Science and Technology: From Concepts to Applications, II Ed, CRC Press, Boca Raton, 2008.

[2] P.J. Blau, Experimental Aspects of friction research on the macroscale, In: Fundamentals of Tribology and Bridging the Gap Between the Macro- and Micro/Nanoscales (ed. B. Bushan), Springer-Science, Dordrecht, 2000, pp. 261-278.

[3] H. Czichos, Technical Diagnostics: Principles, Methods, and Applications, NCSLI Measure 9(2) (2014) 32-40.

[4] A.Grubin, L. Vinogradova, Investigation of the contact of machine components, Central Scientific Research Institute for Technology and Mechanical Engineering, Russia, 1949.

[5] D. Dowson, H. Higginson, Elastohydrodynamic lubrication, I Ed, Pergamon Press, England, 1966.

[6] B. Hamrock, D. Dowson, Isothermal Elastohydrodynamic Lubrication of Point Contacts - Part I, ASME Journal of Lubrication Technology 98(2) (1976) 223-228.

[7] B. Bushan, Principle and Applications of tribology, II Ed., John Wiley & Sons, New York, 2013.

[8] X. Zhang, S. Kanapathipillai, T. Wu, Z. Peng, Friction behavior and friction mechanisms of rolling-sliding contact in mixed EHL, Tribology International 114 (2017) 201-207.

[9] X. Zhang, Z. Li, J. Wang, Friction prediction of rolling-sliding contact in mixed EHL, Measurement 100 (2017) 262-269.

[10] Z. Fu, F. Guo, P. Wong, Friction–speed characteristics of elastohydrodynamically lubricated contacts with anomalous film shapes, Journal of Engineering Tribology 226 (2012) 81-87.

[11] Z. Fu, P. Wong, F. Guo, Effect of Interfacial Properties on EHL Under Pure Sliding Conditions, Tribology Letters 49, 31-38 (2013).

[12] E. Ciulli, K. Stadler, T. Draexl, The influence of the slide-to-roll ratio on the friction coefficient and film thickness of EHD point contacts under steady state and transient conditions, Tribology International 42 (2009) 526-534.

[13] M. Carli, K.J. Sharif, E. Ciulli, Thermal point contact EHL analysis of rolling/sliding contacts with experimental comparison showing anomalous film shapes, Tribology International 42 (2009) 17–525

[14] S. Gunsel, S. Korcek, M. Smeeth, The Elastohydrodynamic Friction and Film Forming Properties of Lubricant Base Oils, Tribology Transactions 42:3 (1999) 559-569

[15] H. Nishikawa, M. Kaneta, Stribeck friction curve in point EHL contacts, Tribology Online 1 (2006) 1-4

[16] J. Hansen, M. Björling, R. Larsson, Topography transformations due to running-in of rolling-sliding non-conformal contacts, Tribology International 144 (2020) 106-126.

[17] J. Hansen, M. Björling, R. Larsson, Mapping of the lubrication regimes in rough surface EHL contacts, Tribology International 131 (2019) 637–651.

[18] M. Björling, R. Larsson, P. Marklund, E. Kassfeldt, Elastohydrodynamic lubrication friction mapping – the influence of lubricant, roughness, speed, and slide-to-roll ratio, Proc. IMechE Part J: J. Engineering Tribology 225 (2015) 671-681.

[19] B. Vengudusamy, C. Enekes, R. Spallek, EHD friction properties of ISO VG 320 gear oils with smooth and rough surfaces, Friction 8(1) (2020) 164–181.

[20] J. Guegan, A. Kadiric, A. Gabelli, H. Spikes, The Relationship Between Friction and Film Thickness in EHD Point Contacts in the Presence of Longitudinal Roughness, Tribology Letters (2016) 64:33.

[21] H. Nishikawa, K. Handa, M. Kaneta, Behavior of EHL films in reciprocating motion, JSME International Journal 38 (1995) 558-567.

[22] Y. Han, J. Wang, W. Li, R. Ma, X. Jin, Oil film variation and surface damage in the process of reciprocation oscillation transformation, Tribology International 140 (2019) 105-128.

[23] B. Vengudusamy, A. Grafl, F. Novotny-Farkas, Comparison of frictional properties of gear oils in boundary and mixed lubricated rolling–sliding and pure sliding contacts, Tribology International 62 (2013) 100-109.

[24] V. Anghel, R.P. Glovnea, H.A. Spikes, Friction and Film-Forming Behaviour of Five Traction Fluids, Journal of Synthetic Lubrication 21 (2004) 13-32.

[25] P. Anderson, Water-lubricated pin-on-disc tests with ceramics, Wear 154 (1992) 37-47.

[26] B. Podgornik, J. Vižintin, S. Jacobson, S. Hogmark, Tribological behaviour of WCyC coatings operating under different lubrication regimes, Surface and Coatings Technology 177 –178 (2004) 558–565.

[27] P.A. Grützmacher, A. Rosenkranz, S. Rammacher, C. Gachot, F. Mücklich, The influence of centrifugal forces on friction and wear in rotational sliding, Tribology International 116 (2017) 256–263.

[28] M. Muller, G. Ostermayer, Measurements of partially lubricated contacts on different scales, PAMM Proc. Appl. Math. Mech 17 (2017) 629-630.

[29] L.Bai, Y. Meng, Z. A. Khan, V. Zhang, The Synergetic Effects of Surface Texturing and MoDDP Additive Applied to Ball‐on‐Disk Friction Subject to Both Flooded and Starved Lubrication Conditions, Tribology Letters (2017) 65:163

[30] A. Kovalchenko, O. Ajayi, A. Erdemir, The effect of laser surface texturing on transitions in lubrication regimes during unidirectional sliding contact, Tribology International 38 (2005) 219-225.

[31] B.Y.C. So, E.E. Klaus, Viscosity-Pressure Correlation of Liquids, ASLE Transactions 23 (1980) 409-421.

[32] S.Y. Li, F. Guo, X.M. Li, C.L. Liu, Elastohydrodynamic Lubrication with Oil Droplets, Tribology Letters (2017) 65:162.

[33] B.J, Hamrock, S.R. Schmid, B.O. Jacobson, Fundamental of Fluid Film Lubrication, II ed., Marcel Dekker, New York, 2004.

[34] ASTM G99-17, “Standard Test Method for Wear Testing with a Pin-on-Disk Apparatus”, ASTM International, West Conshohocken, PA, 2017

[35] G. Stachowiak, A. Batchelor, Engineering Tribology, III ed., Butterworth-Heienmann, Oxford, 2005.

[36] T.E. Tallian, Y. P. Chiu , D. F. Huttenlocher, J. A. Kamenshine, L. B. Sibley, N. E. Sindlinger, Lubricant Films in Rolling Contact of Rough Surfaces, ASLE Transactions 7 (1964) 109-126.

[37] S.Y. Poon, B.Eng., and D. J. Haines, frictional behaviour of lubricated Rolling-contact elements, Proc Instn Mcch Engrs 181 (1966-1967) 363-389

[38] S. Bair, W. O. Winer, Regimes of Traction in Concentrated Contact Lubrication, ASME Transactions 104 (1982) 382-386

[39] W. Wilson, S. Sheu, Effect of Inlet Shear Heating Due to Sliding on Elastohydrodynamic Film Thickness, ASME Journal of Lubrication Technology 105 (1983) 187-188.

[40] M. Masjedi, M.M. Khonsari, On the effect of surface roughness in point-contact EHL: Formulas for film thickness andasperity load. Tribol Int 82(A) (2015) 228–244.

[41] S. Odi-Owei, B.J. Roylance, Traction Behavior in Sliding ehl contacts, Journal of Lubrication Technology 100 (1978) 115-120.

[42] J. Wheeler, P. Vergne, N. Fillot, D. Philippon, On the relevance of analytical film thickness EHD equations for isothermal point contacts: Qualitative or quantitative predictions?, Friction 4 (2016) 369-379.

[43] H. Moes, Communication. In Proceedings of the Symposium on Elastohydrodynamic Lubrication, London, 1965: pp. 244–245.

[44] B. Hamrock, Ball bearing lubrication: The elastohydrodynamics of elliptical contacts, John Wiley & Sons, 1981.

[45] R. Larsson, O. Andersson, Lubricant thermal conductivity and heat capacity under high pressure, Proc. Instn Mech Engrs 214 Part J (2000) 337-342.

[46] Y. Zhang, N. Biboulet, C.H. Venner, A.A. Lubrecht, Prediction of the Stribeck curve under full-film Elastohydrodynamic Lubrication, (in press).

[47] P. Cann, E. Ioannides, B. Jacobsen, A. Lubrecht, The lambda ratio – a critical re-examination, Wear 175 (1994) 177-188.

[48] I. Krupka, P. Sperka, M. Hartl, Effect of surface roughness on lubricant film breakdown and transition from EHL to mixed lubrication, Tribology International 100 (2016) 116-125.

[49] P. Sperka, I. Krupka, M. Hartl, Analytical Formula for the Ratio of Central to Minimum Film Thickness in a Circular EHL Contact, Lubricants (2018) 6-80.

[50] A. Petrousevitch D. Kodnir, R. Salukvadze, D. Bakashvile, The investigation of oil film thickness in lubricated ball-race rolling contact, Wear 19 (1972) 369-389.

[51] C.J. Hooke, The minimum film thickness in lubricated line contacts during a reversal of entrainment-general solution and the development of a design chart, Proc Instn Mech Engrs 208 (1994) 53-64.